A MATERIAL FORCE ANALYSIS OF CRACK GROWTH IN A VISCOELASTIC STRIP

T. D. Nguyen[1] and S. Govindjee[2]

[1]Department of Mechanical Engineering, Mechanics and Computation, Stanford University, CA 94305, USA

[2]Structural Engineering, Mechanics, and Materials, University of California, Berkeley, CA 94720, USA

ABSTRACT

The material force method for inelastic fracture is applied to study steady-state crack growth in a thin viscoelastic strip. The method calculates the work rate of dissipation from a balance of energy momentum that explicitly accounts for the effects of viscoelastic behavior. In a finite element framework, the method provides a tool to visualize the viscous dissipation zone. Simulations of crack growth using inter-element cohesive surfaces was performed for strips of various sizes. The same driving force was applied to each strip. Results show that the finite width of the strip constrains the development of the viscous dissipation zone. There is a critical size of the strip relative to the viscoelastic length scale, calculated by the crack speed and characteristic relaxation time, below which the crack speed exhibits a dependence on geometry.

1 INTRODUCTION

For biological materials composed at least in part of organic polymers such as collagen, proteins, and lipids, viscoelasticity can play an important role in the fracture response. One biological material that has received significant attention in recent years for its extraordinary strength and toughness properties is nacre, the material of the iridescent lining of abalone shells. Nacre is composed of argonite platelets, an orthorhombic calcium carbonate crystal, joined end-to-end to form sheets a few hundred micrometers thick. The sheets are stacked in a staggered formation, and the result is a "brick-and-mortar" microstructure [1]. Nacre displays a toughness that is roughly 3000 times larger than monolithic calcium carbonate, though both materials exhibit similar stiffness properties because of the high volume fraction of the mineral phase in nacre [1]. Gao et. al. [2] proposed that the nanometer size of the argonite crystals in nacre optimizes the strength of the crystals by changing the failure mechanism from Griffith crack growth to uniform decohesion. Crack growth in nacre is restricted then to the soft protein layers which can dissipate significant fracture energy through large deformation and viscoelastic behavior.

In general, viscoelastic behavior in the bulk material generates dissipation which contributes to the fracture energy as measured by the applied loading. The work rate of dissipation typically varies with the crack speed v and scales with the intrinsic fracture energy exhibited by the material under conditions of negligible viscous dissipation. This behavior was recorded for peel tests of adhesive tapes by Gent and Petrich [3] and observed in numerous analytical studies of viscoelastic fracture [4, 5, 6]. Under "small-scale yielding" conditions when viscoelastic behavior is localized to the near-tip region, the fracture energy for a linear material with a single characteristic relaxation time τ varies asymptotically from the intrinsic value to a maximum value that is the intrinsic fracture energy scaled by the ratio ρ of the short-time to long-time moduli . Using scaling analysis, de Gennes [7] proposed that the viscous dissipation zone for steady-state growth occupies a ring $v\tau < r < v\tau/\rho$ surrounding the crack where r is radial distance from the crack tip. The work rate of dissipation produced by a crack growing at speed v depends on the characteristic size of the viscous dissipation ring relative to the characteristic size L of the process region. The effects of viscous dissipation is negligible when the viscous dissipation zone is smaller than the fracture process region. For this case, the fracture

energy equals the intrinsic value. However, the fracture energy acquires its maximum value when the viscous dissipation ring is fully formed outside the process region. For "large-scale yielding" problems where the viscous dissipation region encompasses much of the body, Rahulkumar et. al. [6] showed that the work rate of dissipation depends on the interaction of the viscoelastic parameter $v\tau$ with an additional length scale, the characteristic dimension H of the body. As the boundaries of the viscous dissipation zone grow beyond H, the material response everywhere becomes elastic and the fracture energy decreases to the intrinsic value. Rahulkumar et. al. [6] obtained this result specifically for peeling of a viscoelastic strip. Here, we apply a similar approach to examine the effects of viscoelasticity in the fracture of nacre.

As a first step towards understanding the contribution of viscous dissipation in the protein matrix to the toughness of nacre, we propose to model cohesive crack growth through thin viscoelastic strips of various sizes. The Xu-Needleman cohesive surface model [8] is used to describe the fracture process, and the material force method for inelastic fracture developed by Nguyen et. al. [9] is applied to characterize the geometry of the viscous dissipation zone. The material force method is a path-dependent integral method that calculates the work rate of dissipation independently from the energy release rate. In a finite element framework, the method computes the work rate of dissipation from a field of nodal dissipation forces that can be used to visualize the viscous dissipation zone. Previous analytical studies of viscoelastic fracture have used ad hoc methods to depict the viscous dissipation region. An example developed by Hui et. al. [5] applies a strain parameter that compares the difference between the equivalent strains in the long-time and short-time elastic regions. These methods are approximate because they do not calculate directly the work rate of dissipation.

The first section briefly reviews the material force method for inelastic fracture. The method is applied to the cohesive strip problem to observe the interaction of the viscous dissipation region with the finite boundaries of the strip. We present preliminary results that demonstrates the influence of geometry on the crack speed. Further investigation of these results will help to define the role of viscoelasticity in the fracture of nacre and similar biological materials.

2 Material force method for linear viscoelasticity

This section briefly reviews the development of the material force method for viscoelasticity as presented by Nguyen et. al. [9]. The particular viscoelastic model used in the developments is the generalized standard linear solid. The standard solid model assumes an additive decomposition of the strain into elastic and viscous components, $\boldsymbol{\varepsilon} = \boldsymbol{\varepsilon}^{\mathrm{e}} + \boldsymbol{\varepsilon}^{\mathrm{v}}$. Also assumed is a quadratic free energy density function $\Psi(\boldsymbol{\varepsilon}, \boldsymbol{\varepsilon}^{\mathrm{e}}) = \Psi^{\mathrm{EQ}}(\boldsymbol{\varepsilon}) + \Psi^{\mathrm{NEQ}}(\boldsymbol{\varepsilon}^{\mathrm{e}})$ where $\Psi^{\mathrm{EQ}}(\boldsymbol{\varepsilon})$ is the elastic equilibrium part while $\Psi^{\mathrm{NEQ}}(\boldsymbol{\varepsilon}^{\mathrm{e}})$ denotes the time-evolving nonequilibrium part. The stress response is calculated from the free energy density as, $\boldsymbol{\sigma} = \partial\Psi/\partial\boldsymbol{\varepsilon} = \partial\Psi^{\mathrm{EQ}}/\partial\boldsymbol{\varepsilon} + \partial\Psi^{\mathrm{NEQ}}/\partial\boldsymbol{\varepsilon}^{\mathrm{e}} = \boldsymbol{\sigma}^{\mathrm{EQ}} + \boldsymbol{\sigma}^{\mathrm{NEQ}}$, and a linear evolution equation is prescribed for the viscous strain, $\boldsymbol{\eta} : \dot{\boldsymbol{\varepsilon}}^{\mathrm{v}} = \boldsymbol{\sigma}^{\mathrm{NEQ}}$, where $\boldsymbol{\eta}$ is a positive-definite viscosity tensor. The linear evolution equation is associated with the quadratic viscous dissipation potential $\mathscr{D}^{\mathrm{visc}} = \boldsymbol{\sigma}^{\mathrm{NEQ}} : \dot{\boldsymbol{\varepsilon}}^{\mathrm{v}}$.

Consider the undeformed configuration of a cracked linear viscoelastic body Ω_{o} shown in Fig. 1. The coordinate of a material point in Ω_{o} is denoted by $\mathbf{X}$ while $\mathbf{x}$ is reserved for the spatial coordinates. A contour Γ_{o} with outward unit normal $\mathbf{N}$ is defined about the external boundary and the crack surfaces. Another similarly directed contour Γ_{δ} is drawn around the infinitesimal crack-tip region Ω_{δ} and connected to Γ_{o} to form a closed path. It is assumed that acting on the boundary Γ_{o} is material traction calculated from the projection of the material stress $\boldsymbol{\Sigma}$ onto the surface normal $\mathbf{N}$, and within Ω_{o} are distributed material body forces. Material forces are the thermodynamic conjugates of material motions, the more classical terms of which are configurational changes or inverse motions.
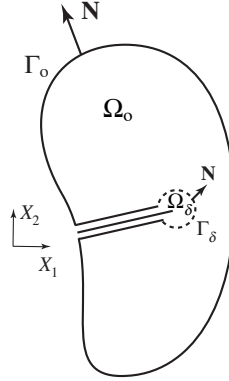
Figure 1: A crack in an otherwise homogeneous body

In an inhomogenous body, distributed material forces are produced by the explicit dependence of the free energy density on the material coordinates $\mathbf{X}$. In a homogeneous body, the presence of material forces also correspond to the motion of defects such as cracks [10, 11], and to inelastic material behavior [10]. Here, we are concerned with the latter two.

For the viscoelastic problem, the material stress is defined in the form of the energy momentum tensor, $\boldsymbol{\Sigma} = \Psi(\boldsymbol{\varepsilon}, \boldsymbol{\varepsilon}^{\mathrm{v}})\mathbf{1} - \boldsymbol{\nabla}\mathbf{u}^{\mathrm{T}}\boldsymbol{\sigma}$, where $\Psi(\boldsymbol{\varepsilon}, \boldsymbol{\varepsilon}^{\mathrm{v}})$ is the free energy density expressed in terms of the total and viscous strain. The associated material viscous body force is given as $\mathbf{f}^{\mathrm{visc}} = \boldsymbol{\sigma}^{\mathrm{NEQ}} : \boldsymbol{\nabla}\boldsymbol{\varepsilon}^{\mathrm{v}}$. The quasistatic material force balance for the volume $\Omega_r = \Omega_{\mathrm{o}} - \Omega_\delta$ in the absence of physical body forces equates the surface and volume forces as,

$$\int_{\Gamma_{\mathrm{o}}} \boldsymbol{\Sigma}\mathbf{N}\,\mathrm{d}S - \lim_{\delta \to 0} \int_{\Omega_r} -\mathbf{f}^{\mathrm{visc}}\,\mathrm{d}V = \lim_{\delta \to 0} \int_{\Gamma_\delta} \boldsymbol{\Sigma}\mathbf{N}\,\mathrm{d}S, \tag{1}$$

where the volume Ω_δ has been shrunk to the crack-tip. The volume term accounts for the aggregate effects of viscoelasticity while the surface term on the right hand side is the material force associated with crack motion. The material force balance also can be obtained directly from the quasistatic equilibrium equation. Within that framework, eqn. (1) acquires the significance of the global balance of energy momentum. In fracture mechanics, the flux of energy-momentum through a contour surrounding the crack-tip is applied by the J-integral to calculated the energy release rate for crack growth.

In the absence of viscoelastic behavior, the volume integral vanishes and the material force balance in eqn. (1) reduces to the path-independence statement of the vectorial J-integral which equates the far-field and near-tip energy-momentum flux. This relation motivates the physical interpretation of the contour integral on the right-hand-side of eqn. (1) as the near-tip free energy release rate. The expression forming the left-hand side is defined as the global material force,

$$\mathbf{F}^{\mathrm{mat}} = \int_{\Gamma_{\mathrm{o}}} \boldsymbol{\Sigma}\mathbf{N}\,\mathrm{d}S - \underbrace{\lim_{\delta \to 0} \int_{\Omega_r} -\mathbf{f}^{\mathrm{visc}}\,\mathrm{d}V}_{\mathbf{F}^{\mathrm{dissip}}}. \tag{2}$$

The global material force $\mathbf{F}^{\mathrm{mat}}$ calculates the difference between the far-field free energy release rate and a volume integral of the viscous body force defined as the global dissipation force $\mathbf{F}^{\mathrm{dissip}}$. The latter is interpreted as the work rate of dissipation in the regular volume Ω_r. Nguyen et. al. [9]

demonstrated this interpretation analytically for steady-state growth. Using numerical examples of cohesive crack growth, they further extended the interpretation to arbitrary transient conditions.

Inspired by Moran and Shih [12], a test function $\mathbf{Q} = Q\mathbf{D}$ is defined for implementation in a finite element setting where $Q = 0$ on the far-field contour Γ_o and $Q = 1$ on the near-tip contour Γ_δ. This test function provides, once approximated using Galerkin shape functions $M_A(\mathbf{X})$, a weak approximation expression for the global material, $\mathbf{F}^{\mathrm{mat},h} = \sum Q_A \mathbf{F}_A^{\mathrm{mat}}$, and dissipation forces, $\mathbf{F}^{\mathrm{dissip},h} = \sum_A \mathbf{F}_A^{\mathrm{dissip}}$, where the nodal material and dissipation forces are assemble from element quantities as,

$$\mathbf{F}_A^{\mathrm{mat}} = \mathop{\mathbf{A}}_{e=1}^{n_{\mathrm{el}}} \int_{\Omega^e} -\mathbf{\Sigma}^h \nabla M_A \, dV - \mathbf{F}_A^{\mathrm{dissip}}, \quad \mathbf{F}_A^{\mathrm{dissip}} = \mathop{\mathbf{A}}_{e=1}^{n_{\mathrm{el}}} - \int_{\Omega^e} \boldsymbol{\sigma}^{NEQ,h} : \nabla \boldsymbol{\varepsilon}^{\mathrm{v,h}} M_A \, dV, \tag{3}$$

Nguyen et. al. [9] applied the material force method to cohesive crack growth in an applied, Mode I K-field. Their results showed that the nodal material forces were significant only in the cohesive zone while the nodal dissipation forces occupied a peanut shaped region around the crack tip. Also unlike the nodal material forces, the nodal dissipation forces were aligned primarily against the direction of crack growth. The global dissipation force calculated according to summation on eqn. (3)b agreed with an independent calculation of the work rate of dissipation. These observations support the interpretation of the global dissipation force as the work rate of dissipation and the region occupied by the nodal dissipation forces as the viscous dissipation zone for cohesive crack growth.
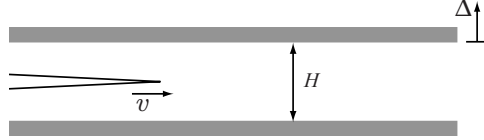
Figure 2: Steady-state growth in infinite viscoelastic strip subjected to fixed displacement loading.

3 Steady-state crack growth in a viscoelastic strip

The infinite strip problem was applied to examine the effects of finite geometry on viscoelastic crack growth. Consider a crack in a thin, infinite viscoelastic strip subjected to fixed displacement loading as shown in Fig. 2. Assuming that viscoelastic deformation is localized to the crack tip region, the far-field energy release rate for steady-state growth can be calculated from the difference in the stored elastic energy of a strip the size of the crack increment δa far ahead of the crack tip and a similar strip far behind the crack tip. The result relates the far-field energy release rate to the width H of the strip and the applied displacement Δ as,

$$G_o = \frac{E^* \Delta^2}{2H}, \tag{4}$$

where for the viscoelastic problem $E^* = E_\infty / (1 - v^2)$ is the plane stress, equilibrium Young's modulus. For the simulations, model viscoelastic parameters were chosen to give $\mu_\infty / \mu_o = 0.5$ for the ratio of the equilibrium and instantaneous shear moduli. The same ratio $\kappa_\infty / \kappa_o = 0.5$ was chosen for the bulk moduli, and the shear and bulk relaxation times were set to unity, $\tau_S = \tau_B = 1$. The values of the equilibrium shear and bulk moduli were selected for a Poisson's ratio of $v = \frac{1}{3}$.
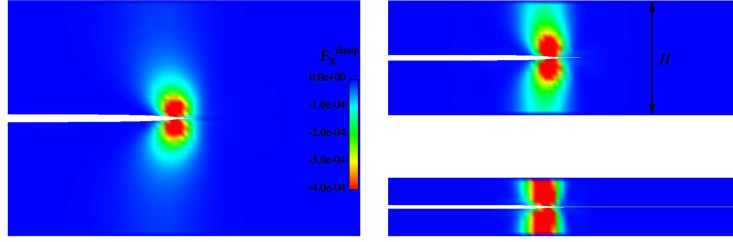
Figure 3: Steady-state viscous dissipation zone for viscoelastic strips of width $H/h = 50, 24, 12$.
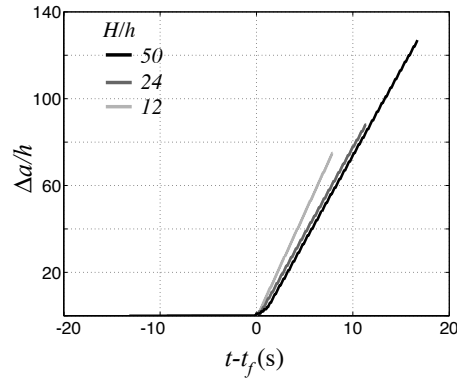
Figure 4: History of crack growth $\Delta a/h$ for viscoelastic strip of various widths

A long, uniform finite element (FE) mesh of square, bilinear elements was used to model the cracked viscoelastic strip. For a given element size, the length of the strip was set to $L = 400h$ and the width of strip was varied in the simulations. Inter-element cohesive surfaces were embedded directly ahead of the precrack for the entire length of the strip. Their constitutive behavior was prescribed by the Xu-Needleman model [8]. The cohesive properties were chosen such that $\delta_n/h = 0.12$ and $\sigma_n = E_\infty/15$ where δ_n and σ_n are the critical crack opening and the peak traction.

Fig. 3 plots the contour of the component of the nodal dissipation forces in the direction of growth for steady-state growth in viscoelastic strips of width $H/h = (50, 24, 12)$. Displacement loading was applied to the strips such that each exhibited the same steady-state, far-field energy release rate as determined from eqn. (4). The assumed values of the far-field energy release rate were verified in the simulation using calculations of the global material force. The contours visualize the viscous dissipation zone which appears for the largest strip as a peanut-shaped region surrounding the crack tip. For the two smaller geometries, the viscous dissipation region grows into the upper and lower boundaries of the strip. Fig. 4 plots the history of crack growth $\Delta a/h$ as a function of time offset by the initiation time t_f. The constant slope displayed by the plots for $t - t_f > 0$ shows that steady-state growth occurs rapidly after initiation. The two larger strips exhibit the same steady-state speed while a faster crack speed is calculated for the smallest strip.

4   Conclusion

A material force method for inelastic fracture was applied to investigate crack growth in a vis-

coelastic strip. In particular, plots of the nodal dissipation force were used to characterize the viscous dissipation zone for steady-state growth in strips of varying widths subjected to the same driving force. The preliminary results presented suggest that below a critical size, the width of the strip constrains the development of the viscous dissipation zone which promotes faster crack growth. In the future, we plan to examine this conclusion by calculating the relationship between the work rate of dissipation and crack speed and by observing more closely the influence of the strip geometry and the cohesive zone on the characteristics of the viscous dissipation zone. We expect that as with the viscoelastic peeling problem studied by Rahulkumar [6], the interaction of the various length scales in the strip problem yields an optimum parameter $v\tau/H$ that maximizes the fracture energy. For biological materials like nacre, comparing this parameter with the length scale of the composite microstructure will clarify the importance of viscoelasticity to the fracture response.

References

[1] Jackson, A. P., Vincent, J. F. V., Turner, R. M., The mechanical design of nacre, Proceedings of the Royal Society of London, Series B 234 (1988) 415–440.

[2] Gao, H., Ji, B., Jäger, I. L., Arzt, E., Fratzl, P., Materials become insensitive to flaws at nanoscale: Lessons from nature, Proceedings of the National Academy of Science 100 (2003) 5597–5600.

[3] Gent, A. N., Petrich, R., Adhesion of viscoelastic materials to rigid substrates, Proceedings of the Royal Society of London, Series A 310 (1969) 433–448.

[4] Shapery, R. A., A theory of crack initiation and growth in viscoelastic media III. Analysis of continuous growth, International Journal of Fracture 11 (1975) 549–562.

[5] Hui, C.-Y., Xu, D. B., Kramer, E. J., A fracture model for a weak interface in a viscoelastic material (small scale yielding analysis), Journal of Applied Physics 72 (1992) 3294–3304.

[6] Rahulkumar, P., Jagota, A., Bennison, S. J., Saigal, S., Cohesive element modeling of viscoelastic fracture: application to peel testing of polymers, International Journal of Solids and Structures 37 (2000) 1873–1897.

[7] De Gennes, P. G., Soft adhesives, Langmuir 12 (1996) 4497–4500.

[8] Xu, X. P., Needleman, A., Numerical simulations of fast crack growth in brittle solids, Journal of the Mechanics and Physics of Solids 42 (1994) 1397–1434.

[9] Nguyen, T. D., Govindjee, S., Klein, P. A., Gao, H., A material force method for inelastic fracture, in review (2003).

[10] Maugin, G. A., Trimarco, C., Psuedomentum and material forces in nonlinear elasticity: variational formulations and application to brittle fracture, Acta Mechanica 94 (1992) 1–28.

[11] Steinmann, P., Application of material forces to hyperelastic fracture mechanics. I. Continuum mechanical setting, International Journal of Solids and Structures 37 (2000) 7371–7391.

[12] Moran, B., Shih, C. F., Crack tip and associated domain integrals from momentum and energy balance, Engineering Fracture Mechanics 27 (1987) 615–642.